A model for describing the light response of the nonphotochemical quenching of chlorophyll fluorescence

Joao Serôdio, Johann Lavaud

A model for describing the light response of the non-photochemical quenching of chlorophyll fluorescence

João Serôdio

Departamento de Biologia and CESAM – Centro de Estudos do Ambiente e do Mar, Universidade de Aveiro, Campus de Santiago, 3810-193, Aveiro, Portugal

Johann Lavaud

UMR CNRS 6250 'LIENSs', Institute for Coastal and Environmental Research (ILE), University of La Rochelle, 2 rue Olympe de Gouges, 17 000 La Rochelle, France

Corresponding author: J. Serôdio

e-mail: jserodio@ua.pt; Tel: +351 234370787; Fax: +351 234372587

Abstract

The operation of photosynthetic energy-dissipating processes is commonly characterised by measuring the light response of the non-photochemical quenching (NPQ) of chlorophyll fluorescence, or NPQ vs. *E* curves. This study proposes a mathematical model for the quantitative description of the generic NPQ vs. *E* curve. The model is an adaptation of the Hill equation and is based on the close dependence of NPQ on the xanthophyll cycle (XC). The model was tested on NPQ vs. *E* curves measured in the plant *Arabidopsis thaliana* and the diatom *Nitzschia palea*, representing the two main types of XC, the violaxanthin-antheraxanthin-zeaxanthin (VAZ) type and the diadinoxanthin-diatoxanthin (DD-DT) type, respectively. The model was also fitted to a large number of published light curves, covering the widest possible range of XC types, taxa, growth conditions, and experimental protocol of curve generation. The model provided a very good fit to experimental and published data, coping with the large variability in curve characteristics. The model was further used to quantitatively compare the light responses of NPQ and of PSII electron transport rate, ETR, through the use of indices combining parameters of the models describing the two types of light-response curves. Their application to experimental and published data showed a systematic large delay of the build-up of NPQ relatively to the saturation of photochemistry. It was found that when ETR reaches saturation, NPQ is on average still below one fifth of its maximum attainable level, which is only reached at irradiances about three times higher. It was also found that organisms having the DD-DT type of XC appeared to be able to start operating the XC at lower irradiances than those of the VAZ type.

Keyword index: Chlorophyll fluorescence; modelling; non-photochemical quenching; photoacclimation; photoprotection; xanthophyll cycle

Introduction

Photosynthesis requires a balance between maximizing light absorption and minimizing damages caused by excessively absorbed light energy. Under natural conditions, exposure to sunlight involves unavoidable risks to the photosynthetic apparatus due to the formation of reactive oxygen species of photosynthetic origin produced under excess light (Osmond et al. 1997; Ort 2001; Demmig-Adams and Adams 2006). The sustainment of prolonged photosynthetic activity under high solar irradiances is ensured by the regulation of the repartition of absorbed light energy between photochemistry and energy-dissipating pathways. The latter function as photoprotective process against permanent damages to the photosynthetic apparatus, or photoinhibition, and are therefore of considerable interest for understanding the resistance of photoautotrophs to environmental stress (Demmig-Adams and Adams 2006; Lavaud 2007; Li et al. 2009).

One of the most important photoprotective processes is the non-photochemical quenching (NPQ). NPQ groups several pathways among which the thermal dissipation of excess energy (or q_E, the energy-dependent quenching, Müller et al., 2001) is considered as the most important. q_E takes place in the light-harvesting antenna of the photosystem II (PS II). It relies on the presence of specific PS II antenna proteins (PsbS in plants, Li et al. 2000; LhcSR in green microalgae, Peers et al. 2009; Lhcx in diatoms, Bailleul et al. 2010), the building of a transthylakoid proton gradient (ΔpH), and the subsequent enzyme-mediated operation (de-epoxidation) of the xanthophyll cycle (XC) (Goss and Jakob, 2010). The XC produces de-epoxidised forms of xanthophylls which are essential regulatory partners of q_E, especially in some groups of microalgae (like the diatoms) (Lavaud, 2007; Li et al. 2009; Goss and Jakob 2010). In plants, green algae and some Heterokontophyta (brown algae, Chrysophyceae), the XC is based on the reversible conversion of pigment violaxanthin (Vx) to the q_E-involved zeaxanthin (Zx), passing through the intermediate form antheraxanthin (Ax) (VAZ type of XC); in other algal groups, like the diatoms, dinoflagellates, Xanthophyceae and Haptophyta, the XC consists in the conversion between only two pigments, diadinoxanthin (DD) and the q_E-involved

diatoxanthin (DT) (DD-DT type of cycle) (Olaizola and Yamamoto 1994; Lavaud et al. 2004; Lavaud 2007). In phycobilisome-containing organisms, there is no XC (cyanobacteria) or its presence is uncertain (red algae) (Goss and Jakob 2010).

The operation of NPQ processes is usually quantified using variable chlorophyll fluorescence (Pulse Amplitude Modulation fluorometry, PAM), by calculating the fluorescence index NPQ, which is based on the relative difference between the maximum fluorescence measured in the dark-adapted state, F_m, and upon exposure to light, F_m' (see Table 1 for notation):

$$\mathrm{NPQ} = \frac{F_m - F_m'}{F_m'} \quad (1)$$

This index is a rearrangement of the Stern-Volmer equation and reflects the assumption that the reciprocal of fluorescence yield is proportional to the Zx or DT concentration (Bilger and Björkman 1990; Lavaud et al. 2002; Baker and Oxborough 2004). The NPQ index has been routinely used to quantify the operation of photoprotective processes as well as the extent of photoinhibitory damages. Under experimental conditions allowing to assume that the prevailing processes causing the quenching of fluorescence are of photoprotective nature, NPQ has been used as a measure of the overall photoprotective capacity of the photosynthetic apparatus (e.g. Dimier et al. 2007b; Lavaud et al. 2007).

One common way to characterise the operation of photoprotective processes or the susceptibility to photoinhibition is to quantify the light response of NPQ. This is done by constructing NPQ vs. *E* curves that record the development of NPQ with increasing incident irradiance. These curves are analogous to the more frequently measured light-response curves of the PSII electron transport rate (ETR) in the sense that they represent the variation of steady state photosynthetic activity between different light levels, thus not informing on the kinetics of NPQ generation, but on the NPQ attainable under each irradiance. The shape of NPQ vs. *E* curve varies widely, both regarding its overall shape as well as the absolute NPQ values

reached. Typically, NPQ increases monotonically with irradiance, varying from zero (measured in darkness) to maximum values that vary greatly with taxonomical groups, physiological state, environmental constraints, or light levels applied. The curve presents a variable degree of sigmoidicity, ranging from cases when NPQ starts to increase steeply from the lowest light levels, following a simple saturation-like pattern (no sigmoidicity), to cases when NPQ remains close to zero for a range of low light levels, then showing an abrupt increase only for intermediate irradiances before stabilizing at maximum values (highly sigmoid). Often, although the stabilization of NPQ is evident, a constant value is not reached within the range of irradiances applied and the maximum attainable NPQ cannot be estimated.

Light-response curves of NPQ have been analysed and interpreted on the basis of arbitrarily chosen features, by qualitatively describing its shape (e.g. low or high sigmoidicity), or by selecting NPQ values reached at particular *E* levels (e.g. NPQ at maximum applied *E*). The absence of an adequate descriptive model impedes the characterization of the curve along the whole range of irradiances applied. Also, the lack of a commonly-used set of descriptive parameters makes it difficult to compare curves measured in different studies or experimental conditions or taxonomic groups.

The present study proposes a simple mathematical model for the quantitative description of the generic NPQ vs. *E* curve, by means of the estimation of a small number of physiologically-meaningful parameters. The model is based on the close, but not absolute, dependence of NPQ on the operation of the XC, through the light-induced de-epoxidation of PS II antenna pigments Vx or DD. To illustrate the main features and variability of the NPQ vs. *E* curve, as well as the interpretation of model parameters, light-response curves were measured on a plant (*Arabidopsis thaliana* (L.); VAZ type XC) and a diatom (*Nitzschia palea* (Kütz) W. Smith; DD-DT type XC) grown under experimental conditions expected to induce a large variability in curve shape and NPQ absolute values. The adequacy of the model was further tested by fitting it to published NPQ vs. *E* curves measured on a large variety of photosynthetic organisms and experimental conditions, and covering the widest possible range of NPQ values and curve shapes. The usefulness of the model was also illustrated by exploring the relationship

between NPQ vs. *E* curves and the photoacclimation status, characterized by light-response curves of the PSII electron transport rate, ETR.

Materials and Methods

Model rationale

The model proposed to describe the light-response curve of NPQ is an adaptation of the Hill equation, originally derived in the context of ligand binding to macromolecules with multiple binding sites. This equation describes the variation of the number of filled binding sites with the increase in ligand concentration, and is routinely used to characterise the cooperativity of enzymatic reactions (Voet and Voet 1990). The use of the Hill equation for modelling the NPQ vs. *E* curve is based on the main assumption that NPQ is mostly due to the operation of the XC coupled to the build-up of the transthylakoid ΔpH, or energy-dependent quenching (q_E; Müller et al. 2001), and that the other potential components of NPQ, the quenching due to state transitions (q_T) or to photoinhibition (q_I) are not expected to significantly affect the NPQ vs. *E* curves (see Discussion). The analogy underlying this rationale is to consider the epoxidized XC pigments Vx and DD as representing the macromolecule of the Hill model, and the transthylakoidal ΔpH-dependent protonation of specific light-harvesting complex (LHC) antenna sites as corresponding to the ligand concentration that bind to their multiple binding sites. At steady state, each irradiance level corresponds to a stable transthylakoidal ΔpH and resulting Vx or DD de-epoxidation and activation through protonation of LHC sites (the so-called 'activation' of Zx and DT; Horton et al. 2000; Goss et al. 2006; Lavaud and Kroth 2006; Horton et al. 2008), and thus to a defined NPQ value. The NPQ vs. *E* curve is thus proposed to be described by the equation:

$$\mathrm{NPQ}\ (E) = \mathrm{NPQ}_{m} \frac{E^{n}}{E_{50}^{n} + E^{n}} \quad (2)$$

where NPQ_m is the maximum NPQ value reached during the light curve, E_{50} is the irradiance level for which NPQ attains 50% of NPQ_m, and n is the Hill coefficient, characterizing the sigmoidicity of the curve. Whilst the parameters E_{50} and n are directly adopted from the Hill equation (originally having only these two parameters), a third parameter, NPQ_m, had to be considered to account for the variability in the absolute values of NPQ. Under the analogy with the ligand binding context of the Hill equation, NPQ(E) is considered to represent the fraction of Vx or DD molecules de-epoxidized into Zx or DT and which have been 'activated'. As such, E_{50} represents the irradiance level necessary to de-epoxidize and 'activate' 50% of convertible Vx or DD pool (ligand concentration resulting in half occupation of binding sites) necessary to reach the maximal NPQ level, NPQ_m. Of potential importance for the characterization of the physiological processes underlying the NPQ vs. E curve is the sigmoidicity parameter n, which measures the type and extent of the reaction cooperativity. In the case of $n < 1$, the curve displays a saturation-like increase asymptotically towards NPQ_m, indicating the presence of a negatively cooperative reaction; if $n > 1$, the curve starts to present a sigmoidal shape, the sigmoidicity increasing with n, indicating a positively cooperative, or allosteric, reaction; if $n = 1$, the model is reduced to the Michaelis-Menten equation, indicative of a non-cooperative reaction.

Measurement of light-response curves

To test the adequacy of the model, Eq. 2 was first fit to NPQ vs. E curves generated for organisms representative of the two types of XC, a plant (*A. thaliana*; VAZ type of XC) and a diatom (*N. palea*; DD-DT type of XC), grown under light conditions expected to induce large variations in NPQ absolute values and in the shape of the NPQ light-response curve. Plants of *A. thaliana* (ecotype Columbia) were grown under controlled growth chamber conditions for 4–

5 weeks under a 16:8 h light/dark cycle and 70% relative humidity. The light/dark temperatures were 22/20 °C. Three irradiance levels were applied: 10 ('low light', LL), 75 ('moderate light', ML) and 150 μmol photons m^{-2} s^{-1} ('high light', HL). The diatom *Nitzschia palea* (Kütz.) W. Smith (collection of the Department of Biology, University of Aveiro) was grown photoautotrophically in unialgal semi-continuous batch 100 mL cultures in sterile natural seawater enriched with f/2 nutrients (Guillard and Ryther 1962). Cultures were grown at 20 °C, under 20 (LL), 100 (ML) and 400 μmol photons m^{-2} s^{-1} (HL) in a 12:12 h light/dark cycle. Cells were harvested by centrifugation (3000 × g, 10 min) during the exponential phase of growth, and were resuspended in fresh growth medium supplemented with $NaHCO_3$ to a final concentration > 10 μg Chl *a* ml^{-1}.

Light-response curves of NPQ and ETR were generated by exposing the samples to 7-12 levels of actinic light, up to 920 μmol m^{-2} s^{-1}. Samples were dark-adapted for 30 min before the start of the light curve to allow determination of fluorescence levels F_o (minimum fluorescence) and F_m, required for the calculation of NPQ (Eq. 1). Samples were light-activated before the start of each light-response curve, through exposure to low light of 54 μmol photons m^{-2} s^{-1} until a steady state in fluorescence was reached (minimum 15 min). Under each light level, a saturation pulse (0.8 s for *A. thaliana* and 0.6 s for *N. palea*) was applied and fluorescence levels F_s (steady state fluorescence) and F_m' were recorded and used to calculate NPQ (Eq. 1) and ETR, using (Genty et al. 1989):

$$\mathrm{ETR} = E \frac{F_m' - F_s}{F_m'} \qquad (3)$$

A different sample (plant leaf or algal culture aliquot) was used for measuring NPQ and ETR under each light level. Three replicated measurements were made for each light level. Light-response curves of ETR were described by fitting the model of Eilers and Peeters (1988), and by estimating the parameters α (the initial slope of the curve), ETR_m (maximum ETR) and E_k (the light-saturation parameter). The parameter E_k is commonly interpreted as a measure of the light

level to which a sample is acclimated to, and commonly used to characterise its photoacclimation status (Behrenfeld et al. 2004).

Chlorophyll fluorescence yield was measured using a PAM fluorometer comprising a computer-operated PAM-Control Unit (Walz) and a WATER-EDF-Universal emitter-detector unit (Gademann Instruments GmbH, Germany), using a modulated blue light (LED-lamp peaking at 450 nm, half-bandwidth of 20 nm) as source for measuring, actinic, and saturating light (Cruz and Serôdio 2008). Fluorescence was measured using a 6 mm-diameter Fluid Light Guide fiberoptics. In the case of *N. palea*, the fiberoptics was connected to a fluorescence cuvette (KS-101, Walz, Effeltrich, Germany).

Published light-response curves

The model was also fitted to published NPQ vs. *E* curves, covering a wide range of taxonomic groups (higher plants, mosses, green algae, diatoms, dinoflagellates, others), XC types (VAZ, DD-DT, absence of XC), mutants with variable degrees of impairment of the XC operation, habitats (land and aquatic higher plants; planktonic and benthic microalgae), growth conditions (e.g. low and high light), physiological state (heat stress or XC inhibitors) and fluorescence light-response curve measuring protocols (steady state and rapid light curves, RLCs). Only species with a known functional XC were considered. Studies presenting light curves having less than seven data points were not considered, because of the large errors in the model fitting and parameter estimation. For each study, when three or more light curves were available for each species and experimental treatment, only the two curves presenting the most extreme (higher and lower) NPQ values were used. Detailed information on the data used in the meta-analysis is summarised in Table 3. When available, the corresponding ETR vs. *E* curves were also characterised by fitting the model of Eilers and Peeters (1988) and by estimating its parameters.

Some studies have reported the formation of NPQ in the dark (Perkins et al. 2010). This phenomenon was observed on diatoms (Jakob et al. 1999) and brown algae (Mouget and

Tremblin 2002), and results in NPQ vs. *E* curves showing a distinctive bi-phasic pattern, with NPQ decreasing from initial high values measured in the dark to a minimum under low to moderate light levels (e.g. Geel et al. 1997; Serôdio et al. 2006). Being relevant only for a limited number of taxonomic groups and physiological conditions, this type of NPQ light-response curve was not considered in the present study.

Model fitting and parameter estimation

The light-response curve models were fitted using a procedure written in Microsoft Visual Basic and based on Microsoft Excel Solver. Model parameters were estimated iteratively by minimizing a least-squares function, forward differencing, and the default quasi-Newton search method. The model can be easily fitted using commonly available software packages. On preliminary tests, this method was compared with the fitting procedures implemented in Sigmaplot 9.0 (Systat Software, Inc., San Jose, USA) and Statistica 8.0 (Statsoft, Inc., Tulsa, USA) and no significant differences were found between the estimates of model parameters.

The standard errors of the parameter estimates were calculated following Ritchie (2008) and are asymptotic standard errors. For nonlinear models such as the one here tested, asymptotic standard errors may not be adequate, as they possibly underestimate the actual parameter uncertainty and cannot evaluate the eventual asymmetry of the confidence regions of estimated parameters (Johnson 2008). A number of alternative approaches exist, the best being based on Monte Carlo methods, such as the Boostrap (Press et al. 1996; Johnson 2008). However, the benefits of pursuing alternative methods, requiring substantially more computation time, depend on the magnitude of the uncertainty associated to parameter estimation. In this study, the use of asymptotic standard errors was justified by the finding that they were on average relatively low, in a majority of cases below 10% of parameter estimates (see below, Results), in which case they can be considered acceptable (Tellinghuisen 2008).

Results

271

272 Model fitting to NPQ vs. *E* curves

273

274 The light-response curves of NPQ measured in the plant *A. thaliana* and in the diatom *N. palea*
275 acclimated to different growth light conditions showed a wide range of curve shapes, varying
276 between two main types: curves with low sigmoidicity, presenting a simple saturation-like
277 pattern (e.g. Fig. 1a, HL), and curves with high sigmoidicity, presenting an initial period of low
278 values, followed by a phase of rapid increase leading to a stage of plateau of maximum values
279 (e.g. Fig. 2a, HL). In all cases, the model provided an excellent fitting to the experimental data
280 throughout the whole range of light levels explaining always more than 99.1% of the data
281 variability (Table 2). Although the residuals (Figs. 1b, 2b) showed in some cases a clearly non-
282 random pattern of variation, values were typically low, between ± 5%. The fitting of the model
283 resulted in a large variation of model parameters with species and growth light conditions,
284 following some consistent trends. Both for *A. thaliana* and *N. palea*, the increase in growth light
285 resulted in an increase in NPQ_m (Fig. 1a, 2a; Table 2). This increase in NPQ_m could be detected
286 despite the fact that in most cases the curves did not reach their maximum values within the
287 range of irradiances applied (e.g. Fig. 1a). Another effect of increasing growth light was the
288 increase in the irradiance level for which the curves reached maximum values. For LL-grown
289 samples, maximum NPQ was reached for lower irradiances, with the curves showing an overall
290 lower sigmoidicity, while for HL-grown samples, curves reached saturation at much higher light
291 levels. This trend could be well described by model parameter E_{50}, which increased with growth
292 light in both species (Table 2).

293 The most noticeable difference between the NPQ light-response curves of *A. thaliana*
294 and *N. palea* was the apparent curve sigmoidicity, with less sigmoid curves being found for the
295 former and more sigmoid curves (and a larger variation) for the latter. This variation in curve
296 sigmoidicity was well characterized by the model parameter *n*, which averaged 1.2 for *A.*
297 *thaliana* (varying from 0.98 to 1.44), whilst reaching an average value of 2.11 for *N. palea*

(varying from 1.61 to 2.61). However, a different pattern of variation was found for each species, with *n* decreasing with growth light in *A. thaliana*, and increasing in *N. palea* (Table 2).

Model fitting to published NPQ vs. *E* curves

The compilation of published light-response curves of NPQ allowed gathering a large number of datasets covering a wide range of NPQ absolute values and curve shapes. The model provided a very good fit to the published data, coping with the large diversity in curve characteristics resulting from different combinations of maximum NPQ values attained (NPQ_m), irradiance range of NPQ build-up (E_{50}), and curve sigmoidicity (*n*) (Table 3). Considering all cases, the model explained more than 96% of data variability, independently of type of XC (and XC impaired mutants), species, growth conditions, and experimental protocol used for the generation of light curves. A summary of the meta-analysis carried out on the data set of published NPQ vs. *E* curves is presented in Table 4. NPQ_m was the most variable parameter (c.v. 112.5%), mostly responding to growth conditions, averaging 2.89 but reaching maximum values above 9 for diatoms and even higher for some mosses (Table 3). E_{50} ranged from 30-40 μmol photons m^{-2} s^{-1} to above 3500 μmol m^{-2} s^{-1}, in all cases attaining values well above growth irradiances (see below). However, with few exception (the diatoms *Skeletonema costatum* and *Phaeocystis antarctica*, and the high light-grown *A. thaliana*), all values of E_{50} above 1200 μmol m^{-2} s^{-1} were obtained for *A. thaliana* mutants with impaired operation of the XC (Table 3). *n* was the least variable parameter (c.v. 50.8%), meaning that the curve shape remained relatively unaltered, and that the variability in the NPQ vs. *E* curves was mainly due to changes in NPQ maximum values and in NPQ onset along the irradiance range. *n* averaged 1.7, corresponding to a noticeable degree of sigmoidicity, although values around 1.0 (no sigmoidicity) or slightly lower (mostly mutants with impaired XC) as well as above 3.0 (very high sigmoidicity) were also found (Table 3).

Despite the low number of data points forming most NPQ vs. *E* curves, standard errors of parameter estimates were on average relatively low (15.6, 27.3 and 12.2% of estimates for

326 NPQ_m, E_{50} and *n*, respectively). However, standard errors were typically much higher in the
327 cases when XC was impaired (24.5, 43.9 and 13.5% for NPQ_m, E_{50} and *n*, respectively),
328 indicating that a high level of precision in the estimation of model parameters can be expected
329 for samples under natural conditions.
330 When comparing different XC types, no clear differences were found between model
331 parameters, due to the large overlap of their range of variation. Model parameters appeared to
332 depend mostly on growth conditions, as larger variations could be found within the same
333 species than amongst different taxonomic groups. The model also described very well the light-
334 response curves of NPQ for composite samples (phytoplankton, microphytobenthos). Model
335 parameters varied independently from each other, as no significant correlations were found
336 between NPQ_m, E_{50} or *n*, either when considering all data pooled together, or when considering
337 for separate for each XC type.
338 Considering the published data, the effects of growth light levels on model parameters
339 were identical to those described for the experimental data of this study. When compared to
340 lower light conditions, NPQ light-response curves of samples acclimated to high light showed
341 higher values of NPQ_m (Bilger and Bjorkman 1990; Burritt and MacKenzie 2003; Müller et al.
342 2004; Ralph and Gademann 2005; Rodríguez-Calcerrada et al. 2007; Cruz and Serôdio 2008)
343 and, with the exception of Ralph and Gademann (2005), all these studies showed a similar
344 increase in E_{50} with growth light. The model also fitted very well the light-response curves of
345 NPQ with impaired functioning of the XC, illustrating the usefulness of estimating model
346 parameters to characterize quantitatively the effects on NPQ of inhibitors (e.g. Bilger and
347 Bjorkman 1990), mutations (e.g. Niyogi et al. 1998), or changes in temperature (Ralph et al.
348 2001).
349 Finally, the model was also found to be adequate to describe NPQ vs. *E* curves
350 generated under non-steady state conditions, i.e. derived from RLCs. The comparison of the
351 model parameters estimated for light curves of different light steps showed the same pattern on
352 VAZ and DD-DT samples, with shorter light steps resulting in lower NPQ_m and higher E_{50},
353 whilst *n* not showing any consistent trend (Ralph and Gademann 2005; Perkins et al. 2006).

354

355 Relationship between NPQ and ETR light-response curves

356

357 To illustrate the application of the model to evaluate to what extent the NPQ response to light is
358 related to the photoacclimation status, the light levels required for induction of NPQ and for
359 photochemistry or ETR saturation were compared. A simple form of achieving this is by the
360 direct comparison of model parameters E_{50} and E_k estimated for the two types of light-response
361 curves. These parameters have the advantage of being measured in the same scale (PAR
362 irradiance, μmol photons m^{-2} s^{-1}) and of being independent of the units used to measure
363 photosynthetic rates, ETR or NPQ, which can vary with the method in use (the case of
364 photosynthesis) or instrument settings (the case of ETR).

365 For the experimental data obtained in this study, the increase in growth irradiance
366 induced a substantial change in the photoacclimation status, noticeable by a clear change in the
367 ETR vs *E* curves. As a result, the increase observed for E_{50} was followed by a similarly large
368 increase in E_k, (due to the decrease of α and the increase of ETR_m), both in *A. thaliana* (Fig. 3)
369 and in *N. palea* (Fig. 4). However, E_{50} was found to be in all cases higher than E_k, by 3.7 and
370 2.5 times, on average, for *A. thaliana* and *N. palea*, respectively (2.90 for the whole data). This
371 result indicates that the light-induced build-up of substantial values of NPQ started only after
372 linear electron transport reached near saturation. Furthermore, it shows that a large fraction of
373 E_{50} variability was related to variations in the photoacclimation status due to different growth
374 light conditions, as E_{50} increased linearly with E_k, both for the plant as for the diatom (although
375 the correlation was not statistical significant, but a clear linear trend is obvious; Fig. 5). This
376 analysis also showed that the slope of the regression line of E_{50} on E_k was higher for *A. thaliana*
377 than for *N. palea*, indicating that, for the same photoacclimation status (the same E_k) the plant
378 requires a higher light level for NPQ to reach 50% of its maximum capacity. Or, in other words,
379 that NPQ is induced latter in the range of irradiances in the plant than in the diatom.

380 Interestingly, the analysis of the subset of published data presenting both NPQ and ETR
381 light-response curves, showed the same generic trend. When pooling together the published and

experimental data for samples with fully operational XC (i.e. excluding mutants or samples treated with XC inhibitors) and E_k estimates based only on steady state light curves (i.e. excluding RLCs as E_k estimation is largely dependent on light step duration; Serôdio et al. 2006), the ratio E_{50}/E_k was found to be higher on organisms having a VAZ type of XC and to differ significantly from those having a DD-DT type (3.32 and 2.39, respectively; *t*-test P = 0.038; Fig. 6a).

Another way to compare the light responses of NPQ and ETR is to calculate the fraction of NPQ that is formed when ETR approaches saturation (i.e. when $E = E_k$), or:

$$NPQ_{Ek} = \frac{NPQ(E_k)}{NPQ_m} \quad (4)$$

Low values of NPQ_{Ek} indicate that when photochemistry saturates, NPQ is still not significantly developed (corresponding to high E_{50}/E_k), whilst high values indicate that NPQ responds more promptly to light increase and the approach of ETR saturation (corresponding to low E_{50}/E_k). Considering both published and experimental data (the data subset used above for comparing E_{50}/E_k), NPQ_{Ek} averaged 0.16, and remained below 0.35, indicating that when $E = E_k$, NPQ hardly reached over one third of the maximum attainable level. Confirming the expected inverted relationship between NPQ_{Ek} and E_{50}/E_k, significantly lower values were found for organisms with a VAZ type of XC than for those with the DD-DT type (0.14 and 0.21, respectively; *t*-test, P = 0.023; Fig. 6b).

Model fitting and parameter estimation

Despite the usually reduced number of data points in the analyzed NPQ light-response curves (average 9.7, maximum 13), the model proposed in this study was found to be easily fitted to experimental curves, in most cases yielding parameter estimates virtually independently from the start values used in the iterative fitting procedure (although realistic start values allows a

more rapid and precise parameter estimation). The main problem found when trying to fit Eq. 2 to NPQ vs. *E* curves occurred when the curves were very close to linear, showing no clear features like sigmoidicity or saturation. This resulted in that a similarly good fit could be reached with different combinations of model parameters values. Still, this occurred only in relatively small number of cases, like the case of the diatom *Skeletonema costatum* (Lavaud et al. 2007) and some *A. thaliana* mutants with severe impairment of XC operation, for which some degree of uncertainty remain associated to the presented parameter estimates.

This problem seems to result from the common situation of having light-response curves constructed with the main purpose of characterizing the ETR vs. *E* curves, NPQ having only a secondary interest. As it often happens that the NPQ approaches its maximum for light levels much above the range used for measuring ETR, the NPQ vs. *E* curve may result truncated and its complete shape may not be available for model fitting. Yet, the relationship established between NPQ and ETR light curves in similar data may be used to impose boundaries to the model parameter estimates, and thus help to reach a single set of meaningful values.

Discussion

Model assumptions

The model proposed for describing the NPQ vs. *E* curve is based on the main assumption that NPQ is mostly due to q_E, the 'energy-quenching' associated to the build-up of the transthylakoid ΔpH and the operation of the XC. This assumption is generally supported by the finding of strong linear relationships between NPQ and de-epoxidized xanthophylls in all groups investigated (plants, green algae, diatoms, Chrysophyceae) and under a wide range of experimental conditions.

However, besides q_E, NPQ also quantifies the fluorescence quenching caused by state transitions (q_T) or by photoinhibition (q_I) which may potentially significantly affect the NPQ vs.

437 *E* curves. q_T is relevant in phycobilisome-containing organisms (cyanobacteria and red algae)
438 (Campbell et al. 1998; Mullineaux and Emlyn-Jones 2004), although not as much in higher
439 plants and green algae (Pfannschmidt 2005; Eberhard et al. 2008; Ruban and Johnson 2009),
440 and it does not occur for the Heterokontophyta (Lavaud 2007). When occurring, q_T is not
441 significant in light conditions triggering q_E-related NPQ (Mullineaux and Emlyn-Jones 2004;
442 Tikkanen et al. 2006; Ruban and Johnson 2009). With the exception of some land plants
443 (overwintering conifers and tropical evergreen species), q_I origin is not clearly defined and it
444 requires particular conditions such as prolonged environmental stress (Müller et al. 2001;
445 Demmig-Adams and Adams 2006; Horton et al. 2008).
446 The effects of q_T or q_I on the light-response curve of NPQ would likely consist in a
447 general change in curve shape, through the increase of NPQ at low light levels (for q_T) and of
448 NPQ_m (for q_I). However, these components of NPQ may be expected not to significantly affect
449 the NPQ vs. *E* curves measured under the usually applied experimental protocols. This is
450 because the duration of the light steps commonly applied ($\leq$ 2-3 min, and much shorter in the
451 case of RLCs) correspond to light doses clearly different than those required to induce both q_T
452 or q_I (Campbell et al. 1998; Müller et al. 2001; Demmig-Adams and Adams 2006; Horton et al.
453 2008; Ruban and Johnson 2009).
454 The same reasoning applies to another implicit assumption of the model, that during the
455 generation of a light curve q_E is due solely to the development of the ΔpH and the subsequent
456 de-epoxidation of the present (and susceptible of being de-epoxidized) pool of xanthophylls. In
457 fact, it is well established that exposure to high light can induce the *de novo* synthesis of XC
458 pigments (e.g. Olaizola and Yamamoto 1994; D'Haese et al. 2004; Lavaud et al. 2004;
459 Demmig-Adams and Adams 2006). This process causes the accumulation of de-epoxidized
460 forms, which could result in the linear increase of NPQ in the high-light part of the curve.
461 Again, the *de novo* synthesis requires the prolonged exposure to very high irradiances (e.g.
462 Lavaud et al. 2004; Demmig-Adams and Adams 2006; Lavaud 2007), well above the light
463 doses applied during the construction of NPQ light-response curves.

Nevertheless, even if significant q_T, q_I or *de novo* pigment synthesis do occur, the resulting curve may still be of the same general shape and describable by the model. In fact, this study showed that the model fits very well to data obtained in a wide range of experimental conditions, in which the occurrence of any of these processes cannot be completely ruled out (Table 3). In this case, however, care should be taken in interpreting and comparing the model parameters estimated for different species or condition, as they may be affected differently by processes other than the build-up of the ΔpH and the XC. In the case of organisms with impaired operation of the XC (mutants or inhibitor-treated samples), the model was nevertheless shown to be of value, providing a useful quantitative characterization of the light response of NPQ.

Another major assumption of the model is that the formation of q_E, through the de-epoxidation of Vx or DD generated by the acidification of the lumen relates to incident irradiance following the generic conditions of application of the Hill equation, i.e. that NPQ can be considered as allosterically regulated by irradiance through the build-up of the transthylakoidal ΔpH. This assumption is partially supported by the finding that, in isolated plant chloroplasts, the regulation of q_E is of allosteric nature, resulting in response curves of q_E as a function of ΔpH of sigmoidal shape, shown to be adequately described by the Hill equation (Pfündel and Dilley 1993; Ruban et al. 2001; Takizawa et al. 2007; Pérez-Bueno et al. 2008). This sigmoidicity is attributed to the protonation of binding sites of the LHC protein *Psbs* induced by lumen acidification, and subsequent conformational changes within the LHC, switching the de-epoxidized xanthophylls to an 'activated' state. It is taken as an indication of allosteric regulation of q_E, resulting from proton binding showing positive cooperativity, and the 'activated' de-epoxidized xanthophylls Zx (Horton et al. 2000; Horton et al. 2008; Li et al. 2009) or DT (Goss et al. 2006; Lavaud and Kroth 2006) acting as a positive effector.

The strong physiological basis of the proposed model is likely to explain its success to cope with a large diversity of light-response curve characteristics. Other mathematical models have also been used to successfully describe NPQ vs. *E* curves, namely an exponential saturation function, the Michaelis-Menten function, and a hyperbolic tangent function (Ritchie

2008). However, these models have only been tested on a reduced dataset, and on light curves of low sigmoidicity. Interestingly, the model that yielded the better fit to experimental data was the Michaelis-Menten equation (Ritchie 2008), a particular case of the model proposed in the present study.

Model fitting to NPQ vs. *E* curves

The usefulness of the model was demonstrated by the possibility to estimate NPQ_m despite the fact that in most cases the curves did not reach a saturation plateau within the range of irradiances applied (e.g. Fig. 1a). When assuming NPQ to represent mostly q_E, the maximum NPQ reached by a sample quantifies its photoprotective potential via the dissipation of excessive light energy. By applying the model, curves measured under different experimental conditions can be readily compared, and changes in NPQ_m (e.g. following changes in growth light conditions) can be quantified, which would be otherwise impossible. The accurate estimation of NPQ_m is also required for quantifying E_{50}, which, in some cases of strict relationship (e.g. for most Heterokontophyta; Lavaud et al. 2004; Lavaud 2007), is interpretable as the light level corresponding to the de-epoxidation and 'activation' of the xanthophyll convertible pool necessary to induce half of the maximal NPQ. The size of the xanthophyll convertible pool can be very different in VAZ and DD-DT organisms varying with species and growth conditions, ranging between 50 and 70% (Lavaud 2007; Goss and Jakob 2010). Again, the fit of Eq. 2 to NPQ vs. *E* curves provided an adequate form of characterizing how promptly the XC is ΔpH-activated when responding to an increase in incident irradiance.

However, while NPQ_m and E_{50} can be grossly estimated by visual inspection of the curves (at least when saturation is reached for the light levels applied), the curve sigmoidicity can hardly be characterized quantitatively without the fit of the model and estimation of *n*. The sigmoidicity coefficient was found to vary around 1.5-2.0, values corresponding to positive cooperativity and thus indicating the allosteric regulation of NPQ by light. Minimum *n* values averaged about 1 (reaching significantly lower values only for cases of XC impairment),

indicate that negative cooperativity is not involved in the regulation of processes underlying NPQ. These results generally support that the allosteric nature known for the more fundamental regulation of q_E by ΔpH in plants (Ruban et al. 2001; Li et al. 2009) holds for the relationship of NPQ to irradiance in a large diversity of photosynthetic organisms.

The Hill coefficient has been interpreted as representing the number of allosteric regulators (D'Haese et al. 2004). Considering the diversity of factors likely to contribute to the NPQ vs. *E* curve (Demmig-Adams and Adams 2006; Eberhard et al. 2008; Horton et al. 2008; Li et al. 2009), some of them not fully identified in some photosynthetic taxa (Lavaud 2007), *n* should be considered simply as an empirical coefficient informing on the degree of allostery and serving as a practical descriptor of the curve shape.

Relationship of NPQ light response to photoacclimation status

The modelling of the NPQ vs. *E* curves opens the new possibility of quantitatively comparing the light responses of NPQ and of photochemistry or ETR. Photosynthesis and ETR light-response curves are very commonly used as a form of characterizing the photoacclimation status of photosynthetic organisms, through the estimation of the parameters of a number of available models (Henley 1993; Behrenfeld et al. 2004; Ralph and Gademann 2005; Guarini and Moritz 2009; Perkins et al. 2010). By describing the NPQ vs. *E* curve by a small set of meaningful parameters, the light response of NPQ can be characterized relatively to the one of ETR or photosynthetic rate.

This possibility is useful for the definition of the light levels corresponding to the onset of NPQ (e.g. activation of the XC) relatively to the saturation of photochemistry. As the light response of NPQ may depend greatly on the photoacclimation status, the characterization and comparison of NPQ vs. *E* curves should be preferably normalized to parameters indicative of photochemistry saturation. Furthermore, the comparison of the NPQ and ETR light responses is also of interest because it provides insight on the way an organism combines the responses of photochemistry and of photoprotective processes to changes in ambient light. However, without

548 adequate parameterization of the NPQ light-response, this question can be answered only
549 approximately.
550 Despite its simplicity, the indices E_{50}/E_k and NPQ_{Ek} here proposed provide an efficient
551 form of comparing the light levels for which NPQ reaches significant values and
552 photochemistry reaches saturation. The application of these indices allowed quantifying the
553 delay of the light response of NPQ relatively to the saturation of photochemistry. Under the
554 assumption that NPQ mostly represents q_E, it showed that it takes about three times the
555 irradiance at E_k for half of q_E to develop and that, at E_k, the formation of q_E is still at relatively
556 low levels, providing typically less than one fifth of maximum photoprotective capacity. For the
557 cases when q_E is strictly related to the XC operation (e.g. in most of Heterokontophyta; Lavaud
558 et al. 2004; Lavaud 2007), the values of the indices E_{50}/E_k and NPQ_{Ek} can be interpreted in
559 terms of the de-epoxidation state of the convertible pool of xanthophylls and their 'activation'
560 upon LHC protonation. Yet, the modelling of the NPQ vs. *E* curve may allow for the
561 development of other indices that better characterize this relationship.
562 Interestingly, the meta-analysis carried out in this study showed consistent differences
563 between the relationships of NPQ light response to photoacclimation status in organisms with
564 VAZ and DD-DT types of XC. The fact that these differences were found despite the diversity
565 in taxa and growth conditions may indicate that they are due to fundamental differences in the
566 way the two types of organisms cope with high light, especially regarding the underlying q_E
567 mechanism and regulation of the XC, illustrating the advantages provided by the quantitative
568 description of the NPQ vs *E* curve.
569
570 **Acknowledgements**
571
572 We thank Glória Pinto, Eleazar Rodriguez and Armando Costa for helping with the seeding of
573 the *Arabidopsis* plants. This study was supported by FCT – Fundação para a Ciência e a
574 Tecnologia, grant SFRH/BSAB/962/2009, to J. Serôdio, by the French consortium CPER-
575 Littoral to J. Lavaud, and by the CNRS – Centre National de la Recherche Scientifique

(programme ‘chercheurs invités’) to both. We thank two anonymous reviewers for critical comments on the manuscript.

References

Baker NR, Oxborough K (2004) Chlorophyll fluorescence as probe of plant photosynthetic productivity. In: Papageorgiou GC and Govindjee (eds) Chlorophyll *a* fluorescence: A signature of photosynthesis. Springer, Dordrecht, pp 65-82

Behrenfeld MJ, Prasil O, Babin M, Bruyant F (2004) In search of a physiological basis for covariations in light-limited and light-saturated photosynthesis. J Phycol 40:4-25

Bailleul B, Rogatoc A, Martino A, Coesel S, Cardol P, Bowler C, Falciatore A, Finazzi G (2010) An atypical member of the light-harvesting complex stress-related protein family modulates diatom responses to light. Proc. Natl. Acad. Sci. USA 107: 18214-18219

Bilger W, Bjorkman O (1990) Role of the xanthophyll cycle in photoprotection elucidated by measurements of light-induced absorbance changes, fluorescence and photosynthesis in leaves of *Hedera canariensis*. Photosynth Res 25:173-185

Burritt DJ, Mackenzie S (2003) Antioxidant metabolism during acclimation of *Begonia* × *erytrophylla* to high light levels. Ann Bot 91:783-794

Campbell D, Hurry V, Clarke AK, Gustafsson P, Gunnar Ö (1998) Chlorophyll fluorescence analysis of cyanobacterial photosynthesis and acclimation. Microbiol Molec Biol Rev 62:667-683

Cosgrove J, Borowitzka M (2006) Applying Pulse Amplitude Modulation (PAM) fluorometry to microalgae suspensions: stirring potentially impacts fluorescence. Photosynth Res 88:343-350

606 Cruz S, Serôdio J (2008) Relationship of rapid light curves of variable fluorescence to
607 photoacclimation and non-photochemical quenching in a benthic diatom. Aquat Bot 88:256-264
608
609 Demmig-Adams B, Adams WW (2006) Photoprotection in an ecological context: the
610 remarkable complexity of thermal energy dissipation. New Phytol 172:11-21
611
612 D'Haese D, Vandermeiren K, Caubergs RJ, Guisez Y, De Temmerman L, Horemans N. (2004)
613 Non-photochemical quenching kinetics during the dark to light transition in relation to the
614 formation of antheraxanthin and zeaxanthin. J Theor Biol 227:175-186
615
616 Dimier C, Corato F, Saviello G, Brunet C (2007a) Photophysiological properties of the marine
617 picoeukaryote *Picochlorum* Rcc 237 (Trebouxiophyceae, Chlorophyta). J Phycol 43:275-283
618
619 Dimier C, Corato F, Tramontano F, Brunet C (2007b) Photoprotection and xanthophyll-cycle
620 activity in three marine diatoms. J Phycol 43:937-947
621
622 Eberhard S, Finazzi G, Wollman F (2008) The dynamics of photosynthesis. Ann Rev Gen
623 42:463-515
624
625 Eilers PH, Peeters JC (1988) A model for the relationship between light intensity and the rate of
626 photosynthesis in phytoplankton. Ecol Model 42:199-215
627
628 Elrad D, Niyogi KK, Grossman AR (2002) A major light-harvesting polypeptide of
629 photosystem II functions in thermal dissipation. Plant Cell 14:1801-1816
630
631 Geel C, Verluis W, Snel JF (1997) Estimation of oxygen evolution by marine phytoplankton
632 from measurement of the efficiency of photosystem II electron flow. Photosynth Res 51:61-70
633

634 Genty B, Briantais JM, Baker NR (1989) The relationship between the quantum yield of
635 photosynthetic electron transport and quenching of chlorophyll fluorescence. Biochim Biophys
636 Acta 990:87–92
637
638 Goss R and Jakob T (2010) Regulation and function of xanthophyll cycle-dependent
639 photoprotection in algae. Photosynth Res In press
640
641 Goss R, Pinto EA, Wilhelm C, Richter M (2006) The importance of a highly active and ΔpH-
642 regulated diatoxanthin epoxidase for the regulation of the PS II antenna function in
643 diadinoxanthin cycle containing algae. J Plant Physiol 163:1008-1021
644
645 Guarini J, Moritz C (2009) Modelling the dynamics of the electron transport rate measured by
646 PAM fluorimetry during Rapid Light Curve experiments. Photosynthetica 47:206-214
647
648 Guillard RRL, Ryther JH (1962) Studies of marine phytoplanktonic diatoms. I. *Cyclotella nana*
649 Hustedt and *Detonula confervaceae* (Cleve) Gran. Can J Microbiol 8:229-239
650
651 Havaux M, Kloppstech K (2001) The protective functions of carotenoid and flavonoid pigments
652 against excess visible radiation at chilling temperature investigated in *Arabidopsis npq* and *tt*
653 mutants. Planta 213:953-966
654
655 Henley WJ (1993) Measurement and interpretation of photosynthetic light-response curves in
656 algae in the context of photoinhibition and diel changes. J Phycol 29:729-739
657
658 Herlory O, Richard P, Blanchard GF (2007) Methodology of light response curves: application
659 of chlorophyll fluorescence to microphytobenthic biofilms. Mar Biol 153:91-101
660

661 Horton P, Ruban AV, Wentworth M (2000) Allosteric regulation of the light-harvesting system
662 of photosystem II. Philos Trans Royal Soc London Series B 355:1361-1370
663
664 Horton P, Johnson MP, Perez-Bueno ML, Kiss AZ, Ruban AV (2008) Photosynthetic
665 acclimation: does the dynamic structure and macro-organisation of photosystem II in higher
666 plant grana membranes regulate light harvesting states? FEBS J. 275:1069-1079
667
668 Jakob T, Goss R, Wilhelm C (1999) Activation of diadinoxanthin de-epoxidase due to a
669 chlororespiratory proton gradient in the dark in the diatom *Phaeodactylum tricornutum*. Plant
670 Biol 1:76-82
671
672 Johnson ML (2008) Nonlinear least-squares fitting methods. In Correia J, Detrich H (eds)
673 Methods in cell biology, vol 84. Elsevier Academic Press, San Diego, pp 781-805
674
675 Jung H-S, Niyogi KK (2009) Quantitative genetic analysis of thermal dissipation in
676 *Arabidopsis*. Plant Physiol 150:977-986
677
678 Kromkamp JC, Dijkman NA, Peene J, Simis SGH, Gons HJ (2008) Estimating phytoplankton
679 primary production in Lake IJsselmeer (The Netherlands) using variable fluorescence (PAM-
680 FRRF) and C-uptake techniques. Eur J Phycol 43:327-344
681
682 Kropuenske LR, Mills MM, Dijken GL, Bailey S, Robinson DH, Welschmeyer NA, Arrigo
683 K.R. (2009) Photophysiology in two major Southern Ocean phytoplankton taxa:
684 Photoprotection in *Phaeocystis antarctica* and *Fragilariopsis cylindrus*. Limnol Oceanogr
685 54:1176-1196
686

687 Krupenina NA, Bulychev AA (2007) Action potential in a plant cell lowers the light
688 requirement for non-photochemical energy-dependent quenching of chlorophyll fluorescence.
689 Biochim Biophys Acta 1767:781–788
690
691 Lavaud J (2007) Fast regulation of photosynthesis in diatoms: mechanisms, evolution and
692 ecophysiology. Funct Plant Sci Biotechnol 1:267-287
693
694 Lavaud J, Kroth PG (2006) In diatoms, the transthylakoid proton gradient regulates the
695 photoprotective non-photochemical fluorescence quenching beyond its control on the
696 xanthophyll cycle. Plant Cell Physiol 47:1010-1016
697
698 Lavaud J, Rousseau B, Etienne AL (2004) General features of photoprotection by energy
699 dissipation in planktonic diatoms (Bacillariophyceae). J Phycol 40:130-137
700
701 Lavaud J, Rousseau B, Gorkom HJ, Etienne A (2002) Influence of the diadinoxanthin pool size
702 on photoprotection in the marine planktonic diatom. Plant Physiol 129:1398-1406
703
704 Lavaud J, Strzepek RF, Kroth PG (2007) Photoprotection capacity differs among diatoms:
705 Possible consequences on the spatial distribution of diatoms related to fluctuations in the
706 underwater light climate. Limnol Oceanogr 52:1188-1194
707
708 Li X-P, Björkman O, Shih C, Grossman AR, Rosenquist M, Jansson S, Niyogi KK (2000) A
709 pigment-binding protein essential for regulation of photosynthetic light harvesting. Nature
710 403:391-395
711
712 Li Z, Wakao S, Fischer BB, Niyogi KK (2009) Sensing and responding to excess light. Annu
713 Rev Plant Biol 60:239-260
714

715 Lokstein H, Tian L, Polle JE, DellaPenna D (2002) Xanthophyll biosynthetic mutants of
716 *Arabidopsis thaliana*: altered nonphotochemical quenching of chlorophyll fluorescence is due to
717 changes in Photosystem II antenna size and stability. Biochim Biophys Acta 1553:309-319
718
719 Marschall M, Proctor MCF (2004) Are bryophytes shade plants? Photosynthetic light responses
720 and proportions of chlorophyll *a*, chlorophyll *b* and total carotenoids. Ann Bot 94:593-603
721
722 Mouget J-L, Tremblin G (2002) Suitability of the Fluorescence Monitoring System (FMS,
723 Hansatech) for measurement of photosynthetic characteristics in algae. Aquat Bot 74:219-231
724
725 Mullineaux CW, Emlyn-Jones D (2005) State transitions: an example of acclimation to low-
726 light stress. J Exp Bot 56:389-393
727
728 Müller P, Li X-P, Niyogi KK (2001) Non-photochemical quenching. A response to excess light
729 energy. Plant Physiol 125:1558-1566
730
731 Müller-Moulé P, Conklin PL, Niyogi KK (2002) Ascorbate deficiency can limit violaxanthin
732 de-Epoxidase activity in vivo. Plant Physiol 128:970-977
733
734 Müller-Moulé P, Golan T, Niyogi KK (2004) Ascorbate-deficient mutants of Arabidopsis grow
735 in high light despite chronic photooxidative stress. Plant Physiol 134:1163-1172
736
737 Munekage Y, Hojo M, Meurer J, Endo T, Tasaka M, Shikanai T (2002) *PGR5* is involved in
738 cyclic electron flow around photosystem I and is essential for photoprotection in *Arabidopsis*.
739 Cell 110:361-371
740

741 Munshi MK, Kobayashi Y, Shikanai T (2006) Chlororespiratory Reduction 6 is a novel factor
742 required for accumulation of the chloroplast NAD(P)H dehydrogenase complex in Arabidopsis.
743 Plant Physiol 141:737-744
744
745 Niyogi KK, Grossman AR, Björkman O (1998) Arabidopsis mutants define a central role for
746 the xanthophyll cycle in the regulation of photosynthetic energy conversion. Plant Cell 10:1121-
747 1134
748
749 Olaizola M, Yamamoto HY (1994) Short-term response of the diadinoxanthin cycle and
750 fluorescence yield to high irradiance in *Chaetoceros muelleri* (Bacillariophyceae). J Phycol
751 30:606-612
752
753 Ort DR (2001) When there is too much light. Plant Physiol 125:29–32
754
755 Osmond B, Badger M, Maxwell K, Björkman O, Leegood R (1997) Too many photons:
756 photorespiration, photoinhibition and photooxidation. Trends Plant Sci 2:119-121
757
758 Peers G, Truong TB, Ostendor E, Busch A, Elrad D, Grossman AR, Hippler M,. Niyogi KK
759 (2009) An ancient light-harvesting protein is critical for the regulation of algal photosynthesis.
760 Nature 462:518-522
761
762 Pérez-Bueno ML, Johnson MP, Zia A, Ruban AV, Horton P (2008) The Lhcb protein and
763 xanthophyll composition of the light harvesting antenna controls the ΔpH-dependency of non-
764 photochemical quenching in *Arabidopsis thaliana*. FEBS Lett 582:1477-1482
765
766 Perkins RG, Kromkamp J, Serôdio J, Lavaud J, Jesus B, Mouget J-L, Forster R, Lefebvre S
767 (2010) The application of variable chlorophyll fluorescence to microphytobenthic biofilms. In:
768 Suggett D, Prasil O, Borowitza MA (eds) Chlorophyll *a* Fluorescence in Aquatic Sciences:

Methods and Applications. Developments in Applied Phycology 4. Springer, Dordrecht, pp 273-275

Perkins RG, Mouget J-L, Lefebvre S, Lavaud J (2006) Light response curve methodology and possible implications in the application of chlorophyll fluorescence to benthic diatoms. Mar Biol 149:703-712

Pfannschmidt T (2005) Acclimation to varying light qualities: toward the functional relationship of state transitions and adjustment of photosystem stoichiometry. J Phycol 41:723-725

Pfündel EE, Dilley RA (1993) The pH dependence of violaxanthin deepoxidation in isolated pea chloroplasts. Plant Physiol 101:65-71

Press WH, Teukolsky S, Vetterling W, Flannery B (1996) Numerical recipes in Fortran 90. The Art of Parallel Scientific Computing. 2nd ed Cambridge University Press, Cambridge

Ralph PJ, Gademann R (2005) Rapid light curves: a powerful tool to assess photosynthetic activity. Aquat Bot 82:222-237

Ralph PJ, Gademann R, Larkum AW (2001) Zooxanthellae expelled from bleached corals at 33 ºC are photosynthetically competent. *Marine Ecology Progress Series* 220:163-168

Ritchie RJ (2008) Fitting light saturation curves measured using modulated fluorometry. Photosynth Res 96:201-215

Rodríguez-Calcerrada J, Pardos JA, Gil L, Aranda I (2007) Acclimation to light in seedlings of *Quercus petraea* (Mattuschka) Liebl. and *Quercus pyrenaica* Willd. planted along a forest-edge gradient. Trees 21:45-54

Ruban AV, Johnson MP (2009) Dynamics of higher plant photosystem cross-section associated with state transitions. Photosynth Res 99:173-183

Ruban AV, Wentworth M, Horton P (2001) Kinetic analysis of nonphotochemical quenching of chlorophyll fluorescence. 1. Isolated chloroplasts. Biochemistry 40:9896-9901

Serôdio J, Vieira S, Cruz S, Coelho H (2006) Rapid light-response curves of chlorophyll fluorescence in microalgae: relationship to steady-state light curves and non-photochemical quenching in benthic diatom-dominated assemblages. Photosynth Res 90:29-43

Takizawa K, Cruz JA, Kanazawa A, Kramer DM (2007) The thylakoid proton motive force *in vivo*. Quantitative, noninvasive probes, energetics, and regulatory consequences of light-induced *pmf*. Biochim Biophys Acta 1767:1233–1244

Tellinghuisen J (2008) Stupid statistics! In Correia J, Detrich H (eds) Methods in cell biology, vol 84. Elsevier Academic Press, San Diego, pp 739-780

Tikkanen M, Pippo M, Suorsa M, Sirpio S, Mulo P, Vainonen J, Vener A, Allahverdiyeva Y, Aro EM (2006) State transitions revisited - a buffering system for dynamic low light acclimation of Arabidopsis. Plant Molec Biol 62:779-793

Voet D, Voet JG (1990) Biochemistry. John Wiley and Sons, New York

Table 1. Notation

α – Initial slope of the ETR vs. *E* curve

Ax – Antheraxanthin

DD – Diadinoxanthin

DT – Diatoxanthin

E – PAR irradiance (µmol photons m^{-2} s^{-1})

E_{50} – Irradiance level corresponding to 50% of NPQ_m in a NPQ vs. *E* curve

E_k – Light-saturation parameter of the ETR vs. *E* curve

ETR – PSII relative electron transport rate

ETR_m – Maximum ETR in a ETR vs. *E* curve

F_o, F_m – Minimum and maximum fluorescence of a dark-adapted sample

F_s, F_m' – Steady state and maximum fluorescence of a light-adapted sample

NPQ – Non-photochemical quenching

NPQ_m – Maximum NPQ value reached in a NPQ vs. *E* curve

NPQ_{Ek} – Fraction of NPQ_m reached when $E = E_k$

n – Sigmoidicity coefficient of the NPQ vs. *E* curve

PSII – Photosystem II

RLC – Rapid light-response curve

VAZ – Vx-Ax-Zx XC

Vx – Violaxanthin

XC – Xanthophyll cycle

Zx – Zeaxanthin

Table 2. Summary of the results of the fitting of the model to NPQ vs. *E* curves measured in *A. thaliana* and *N. palea* grown under low (LL), moderate (ML) and high light (HL). Parameter estimates ± one standard error.

		Model parameters			
		NPQ_m	E_{50}	n	r^2
A. thaliana	LL	3.91 ± 0.82	209.9 ± 8.31	1.44 ± 0.52	0.999
	ML	4.63 ± 0.24	542.0 ± 49.2	1.21 ± 0.04	0.999
	HL	5.90 ± 1.04	1141.0 ± 372.1	0.98 ± 0.06	0.998
N. palea	LL	2.70 ± 0.10	91.7 ± 7.01	1.61 ± 0.19	0.991
	ML	3.65 ± 0.05	312.6 ± 5.59	2.16 ± 0.05	0.999
	HL	3.86 ± 0.11	551.4 ± 15.8	2.55 ± 0.08	0.999

Table 3. Results of fitting of Eq. 2 to published NPQ vs. *E* curves. Composite: samples containing organisms with different XC types. LC: light curve protocol (SS: steady state LL; RLCx: rapid light curve, x seconds light step; N-SLC: non-sequential light curve). Treatment: conditions applied before the measurement of the light curves (PAR, temperature); growth conditions when more than one curve available for the same taxon (HL: high light; LL: low light; DTT: XC inhibitor dithiothreitol; LL/HL: transfer from LL to HL; Dense: plants from dense forest stand; Edge: plants from forest edge; IL: intermittent light; CL: continuous light; wt: wild type; *aba1*, *crr6*, *CRR6*, *lut1*, *lut2*, *lut2*, *npq1*, *npq2*, *npq4*, *npq5*, *vtc2*: mutants; LI-1, Sf-2, Col-0, Ws-2: *Arabidopsis* accessions; Mixing: water column mixing). Parameter estimates ± one standard error.

					Model parameters				
XC type	Taxon		LC	Treatment	NPQ_m	E_{50}	n	r^2	Reference
VAZ	Magnoliophyta (flowering plants)	*Arabidopsis thaliana*	SS	wt 10 ºC	2.07 ± 0.04	113.6 ± 6.0	1.11 ± 0.08	0.998	Havaux and Kloppstech (2001)
				wt 25 ºC	2.98 ± 0.40	1118.0 ± 293.8	1.09 ± 0.11	0.996	
				npq1 10 ºC	1.68 ± 0.25	636.5 ± 587.0	0.40 ± 0.06	0.998	
				npq1 25 ºC	1.16 ± 0.22	867.1 ± 557.5	0.63 ± 0.10	0.995	
			SS	Li-1	3.76 ± 0.18	563.8 ± 40.6	1.83 ± 0.16	0.998	Jung and Niyogi (2009)
				Sf-2	4.12 ± 0.16	661.9 ± 33.7	2.03 ± 0.13	0.999	
				Col-0	3.29 ± 0.19	683.7 ± 55.0	1.84 ± 0.16	0.998	
				Ws-2	3.32 ± 0.19	599.8 ± 49.1	1.96 ± 0.21	0.997	
			SS	wt	2.06 ± 0.08	184.1 ± 13.4	2.21 ± 0.32	0.993	Lokstein et al. (2002)
				lut1	1.52 ± 0.06	195.5 ± 13.7	2.28 ± 0.33	0.994	
				lut2	1.76 ± 0.10	231.0 ± 22.2	1.72 ± 0.22	0.995	
				aba1	2.36 ± 0.19	251.1 ± 43.2	1.14 ± 0.13	0.996	
				lut2aba1	1.17 ± 0.07	214.7 ± 30.6	1.08 ± 0.10	0.997	

	SS	wt	3.22 ± 0.22	822.2 ± 90.9	1.46 ± 0.15	0.993	Müller-Moulé et al. (2002)
		vtc2	3.86 ± 0.22	1606.8 ± 137.5	1.32 ± 0.05	0.957	
	SS	wt LL	2.99 ± 0.22	993.6 ± 96.6	1.95 ± 0.21	0.998	Müller-Moulé et al. (2004)
		vtc2 LL	4.52 ± 1.08	2492.1 ± 700.8	1.49 ± 0.15	0.999	
		vtc2npq4 LL	2.03 ± 0.32	2556.4 ± 402.8	1.73 ± 0.08	0.991	
		vtc2npq1 LL	2.51 ± 1.41	2597.0 ± 1777.5	1.43 ± 0.26	0.998	
		wt HL	4.55 ± 6.55	4082.0 ± 5997.8	1.47 ± 0.37	0.998	
		vtc2 HL	6.82 ± 2.35	4133.0 ± 1851.3	1.24 ± 0.10	0.999	
		vtc2npq4 HL	1.82 ± 1.00	3527.3 ± 2314.0	1.39 ± 0.21	0.996	
		vtc2npq1 HL	1.80 ± 1.84	3502.8 ± 4087.1	1.39 ± 0.32	0.996	
	SS	wt	2.21 ± 0.10	457.0 ± 26.5	1.48 ± 0.16	0.993	Munekage et al. (2002)
		pgr5	1.77 ± 3.20	1478.1 ± 5634.7	0.81 ± 0.45	0.957	
	SS	wt	2.25 ± 0.11	503.2 ± 39.4	1.44 ± 0.07	0.999	Munshi et al. (2006)
		crr6	2.00 ± 0.07	397.7 ± 22.5	1.60 ± 0.08	0.999	
		crr6CRR6	2.01 ± 0.08	365.2 ± 24.2	1.65 ± 0.11	0.999	
	SS	wt	4.47 ± 1.24	1894.4 ± 746.9	1.34 ± 0.17	0.995	Niyogi et al. (1998)
		npq1	1.92 ± 0.81	1877.4 ± 1686.5	0.90 ± 0.18	0.988	
		npq2	3.23 ± 0.35	1156.2 ± 207.4	1.32 ± 0.11	0.997	
Begonia× erythrophylla	SS	LL	1.27 ± 0.04	388.3 ± 14.1	3.51 ± 0.36	0.992	Burritt and Mackenzie (2003)
		LL/HL	1.77 ± 0.05	467.3 ± 15.8	2.95 ± 0.23	0.997	
		HL	2.83 ± 0.17	618.3 ± 38.6	2.82 ± 0.32	0.995	
Hedera canariensis	SS	LL	3.61 ± 0.04	382.6 ± 6.3	2.90 ± 0.13	0.999	Bilger and Björkman (1990)
		LL+DTT	1.14 ± 0.18	656.2 ± 218.9	1.09 ± 0.20	0.987	
		HL	5.34 ± 0.33	761.1 ± 59.6	2.05 ± 0.24	0.996	
		HL+DTT	1.48 ± 0.05	437.0 ± 27.8	2.20 ± 0.26	0.994	
Quercus petraea	SS	Dense	2.23 ± 0.03	158.2 ± 6.35	1.83 ± 0.13	0.998	Rodríguez-Calcerrada et al. (2007)
		Edge	5.55 ± 0.11	423.2 ± 13.3	2.04 ± 0.10	0.999	

		Zostera marina	SS	LL	0.87 ± 0.15	797.3 ± 302.0	1.01 ± 0.14	0.995	Ralph and Gademann (2005)
			SS	HL	3.12 ± 0.25	400.5 ± 65.3	1.30 ± 0.16	0.995	
			RLC5	HL	1.36 ± 0.06	276.9 ± 26.9	1.39 ± 0.17	0.997	
			RLC10	HL	2.34 ± 0.17	399.0 ± 60.7	1.02 ± 0.11	0.997	
			RLC40	HL	3.37 ± 0.15	360.7 ± 30.4	1.45 ± 0.12	0.998	
	Bryophyta (mosses)	*Eurhynchium crassinervium*	SS		5.79 ± 0.58	237.9 ± 34.7	1.53 ± 0.12	0.998	Marschall and Proctor (2004)
		Pogonatum urnigerum			5.45 ± 0.48	584.7 ± 65.2	1.79 ± 0.15	0.998	
		Polytrichum juniperinum			5.90 ± 0.34	689.3 ± 34.3	2.68 ± 0.17	0.998	
		Tortula (Syntrichia) ruralis			12.23 ± 0.42	458.6 ± 16.5	2.61 ± 0.15	0.999	
		Racomitrium aquaticum			26.27 ± 3.23	830.8 ± 92.8	2.33 ± 0.18	0.999	
		Trichocolea tomentella			1.45 ± 0.06	68.7 ± 4.5	2.36 ± 0.33	0.992	
	Chlorophyta (green algae)	*Chara corallina*	SS		1.67 ± 0.04	34.0 ± 0.5	6.80 ± 0.73	0.993	Krupenina and Bulychev (2007)
		Chlamydomonas reinhardtii	SS	wt	1.83 ± 1.46	1010.0 ± 1660.0	0.81 ± 0.15	0.992	Elrad et al. (2002)
				npq5	0.19 ± 0.01	56.2 ± 3.58	3.66 ± 0.74	0.986	
		Picochlorum sp.	SS		1.88 ± 0.29	410.2 ± 142.0	1.06 ± 0.20	0.975	Dimier et al. (2007a)
	Eustigmatophyceae	*Nannochloropsis oculata*	RLC10		1.01 ± 0.06	224.5 ± 31.7	1.01 ± 0.08	0.998	Cosgrove and Borowitzka (2006)
DD-DT	Bacillariophycea (diatoms)	*Chaetoceros socialis*	SS		5.71 ± 0.08	149.4 ± 4.8	1.88 ± 0.10	0.999	Dimier et al. (2007b)
		Skeletonema marinoi			1.27 ± 0.03	233.0 ± 9.3	1.95 ± 0.13	0.998	
		Thalassiosira rotula			1.14 ± 0.18	198.9 ± 89.8	0.89 ± 0.23	0.977	
		Fragilariopsis cylindrus	SS	5 µmol m^{-2} s^{-1}	1.00 ± 0.18	637.5 ± 266.1	1.08 ± 0.23	0.966	Kropuenske et al. (2009)
				65 µmol m^{-2} s^{-1}	0.74 ± 0.08	1023.1 ± 233.6	1.05 ± 0.9	0.996	
				125 µmol m^{-2} s^{-1}	0.59 ± 0.12	1024.5 ± 540.6	0.94 ± 0.13	0.986	
		Phaeodactylum tricornutum	SS		2.30 ± 0.10	367.6 ± 24.1	2.59 ± 0.45	0.984	Lavaud et al.

		Skeletonema costatum			2.77 ± 0.75	2825.9 ± 1569.0	0.86 ± 0.08	0.998	(2007)
		Thalassiosira. oceanica			0.88 ± 0.13	859.4 ± 282.2	0.95 ± 0.13	0.992	
		Thalassiosira pseudonana			1.05 ± 0.04	276.8 ± 18.4	1.96 ± 0.22	0.993	
		Thalassiosira weissflogii			1.58 ± 0.03	227.1 ± 8.3	2.70 ± 0.22	0.996	
		Phaeodactylum tricornutum	SS	IL	9.30 ± 0.10	288.5 ± 6.2	2.77 ± 0.16	0.999	Lavaud et al.
				CL	2.16 ± 0.08	334.4 ± 17.2	3.22 ± 0.71	0.980	(2002)
		Navicula phyllepta	RLC10		0.19 ± 0.06	1057.6 ± 731.3	1.01 ± 0.36	0.976	Perkins et al.
			RLC30		0.54 ± 0.07	972.2 ± 370.1	0.73 ± 0.11	0.997	(2006)
			RLC60		0.91 ± 54.5	450.0 ± 54.5	1.55 ± 0.28	0.990	
			SS		2.90 ± 0.57	1152.8 ± 463.0	1.10 ± 0.26	0.989	
		Nitzschia palea	SS	LL	3.48 ± 0.17	115.8 ± 12.2	1.38 ± 0.15	0.991	Cruz and
				HL	5.62 ± 0.24	399.9 ± 27.1	1.58 ± 0.08	0.999	Serôdio (2008)
	Dinophyta (dinoflagellates)	*Symbiodinium* sp.	RLC5	25 °C	0.15 ± 0.01	143.3 ± 10.5	2.39 ± 0.32	0.996	Ralph et al.
				33 °C	0.53 ± 0.05	115.8 ± 22.5	1.21 ± 22.5	0.994	(2001)
				37 °C	1.20 ± 0.05	77.3 ± 6.7	1.18 ± 0.08	0.998	
				38 °C	0.37 ± 0.01	39.9 ± 2.2	1.66 ± 0.17	0.995	
	Haptophyta	*Phaeocystis antarctica*	SS	5 µmol m^{-2} s^{-1}	0.27 ± 0.03	426.7 ± 49.7	1.93 ± 0.29	0.990	Kropuenske et
				65 µmol m^{-2} s^{-1}	1.49 ± 1.01	2953.0 ± 3309.0	1.07 ± 0.27	0.985	al. (2009)
				125 µmol m^{-2} s^{-1}	0.84 ± 0.13	755.1 ± 175.0	1.94 ± 0.56	0.986	
Composite		Microphytobenthos	RLC50		4.09 ± 0.12	349.2 ± 17.8	2.39 ± 0.26	0.994	Herlory et al.
			N-SLC		3.72 ± 0.13	546.2 ± 35.5	1.49 ± 0.10	0.996	(2007)
		Phytoplankton	SS	No mixing	5.07 ± 0.52	546.6 ± 85.5	1.42 ± 0.13	0.998	Kromkamp et
				Mixing	1.85 ± 0.09	446.4 ± 21.9	2.73 ± 0.24	0.997	al. (2008)

857

858

Table 4. Summary of the meta-analysis of the results of the fitting of the model to published NPQ vs. *E* curves (listed in Table 3). Mean values ± one standard error.

	Model parameters		
XC type	NPQ_m	E_{50}	n
VAZ	3.30 ± 0.49	926.7 ± 135.1	1.77 ± 0.13
DD-DT	1.88 ± 0.41	657.9 ± 145.9	1.60 ± 0.14
Mixed	3.68 ± 0.67	472.1 ± 47.3	2.01 ± 0.33
All	2.89 ± 0.35	824.3 ± 99.2	1.73 ± 0.09

Figure legends

Fig. 1. Fitting of Eq. 2 to light-response curves of NPQ measured in the plant *A. thaliana* grown under low (LL), moderate (ML) and high light (HL). a. Light-response curves (data points), fitted model (lines), and estimates of model parameters. b. Residuals of the model fitting.

Fig. 2. Fitting of Eq. 2 to light-response curves of NPQ measured in the diatom *N. palea* grown under low (LL), moderate (ML) and high light (HL). a. Light-response curves (data points), fitted model (lines), and estimates of model parameters. b. Residuals of the model fitting.

Fig. 3. Comparison between the light-response curves of NPQ and of ETR of *A. thaliana* grown under low (LL), moderate (ML) and high light (HL). Estimates of the parameters of the model of Eilers and Peeters (1988) fitted to the ETR vs. *E* curves are presented. Estimates of the parameters of the curves fitted to the NPQ vs. *E* curves are presented in Table 2.

Fig. 4. Comparison between the light-response curves of NPQ and ETR of *N. palea* grown under low (LL), moderate (ML) and high light (HL). Estimates of the parameters of the model of Eilers and Peeters (1988) fitted to the ETR vs. *E* curves are presented. Estimates of the parameters of the curves fitted to the NPQ vs. *E* curves are presented in Table 2.

Fig. 5. Relationship between the parameter E_{50} of Eq. 2 fitted to the NPQ vs. *E* curves and the parameter E_k of the Eilers and Peeters (1988) model fitted to the ETR vs. *E* curves, for the plant *A. thaliana* (circles) and the diatom *N. palea* (squares) grown under high (white), moderate (gray) and low light (black).

Fig. 6. Comparison between the ratios E_{50}/E_k (a) and $NPQ(E_k)/NPQ_m$ (b) as calculated for the published (excluding cases with impaired XC operation) and experimental (this study) light-

response curves of NPQ and ETR in VAZ and DD-DT types of XC. Bars represent one standard error, boxes represent the lower (25%) and upper (75%) quartiles, and the thin and thick horizontal lines inside the boxes represent the mean and the median, respectively.

895 Figure 1

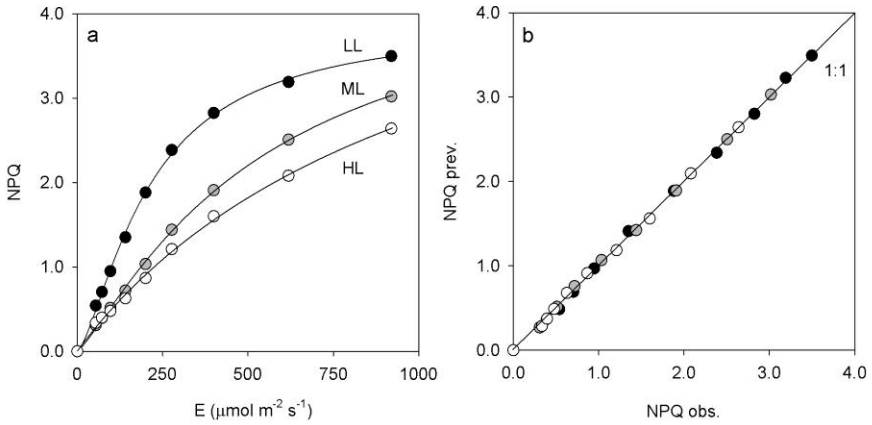

896

897

898

899 Figure 2

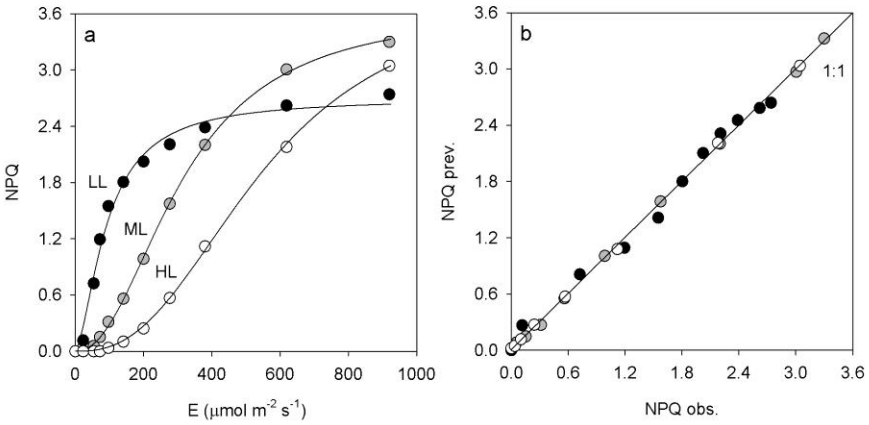

900

901

902 Figure 3

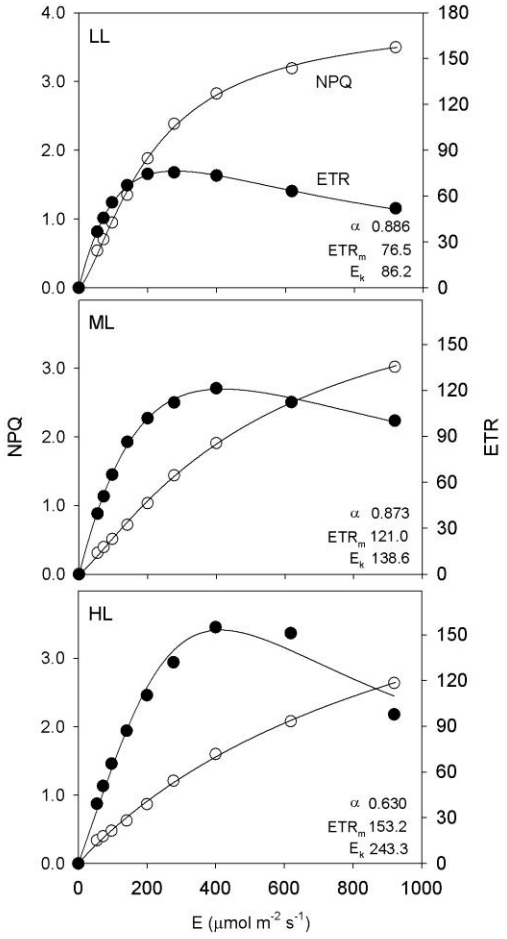

903

904

905 Figure 4

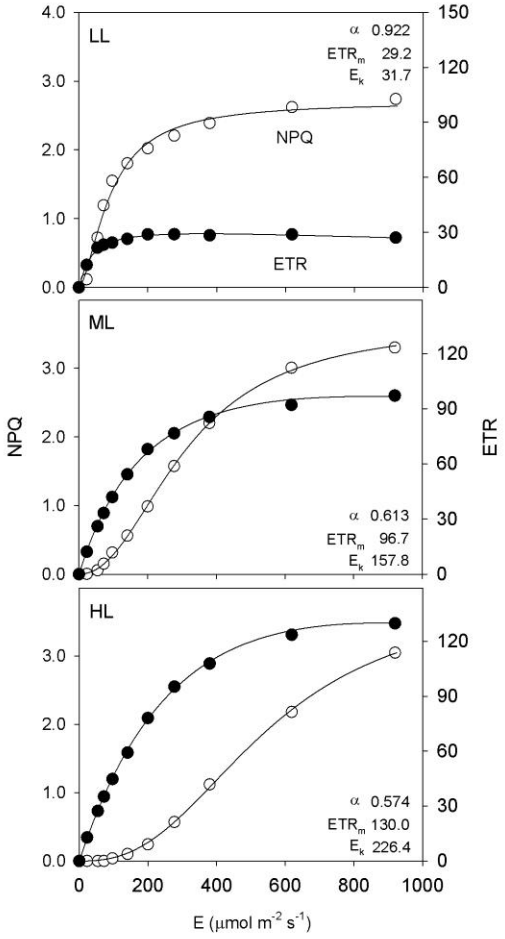

906

907

908 Figure 5

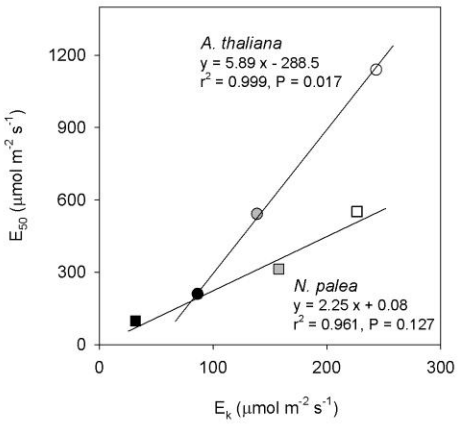

909

910

911 Figure 6

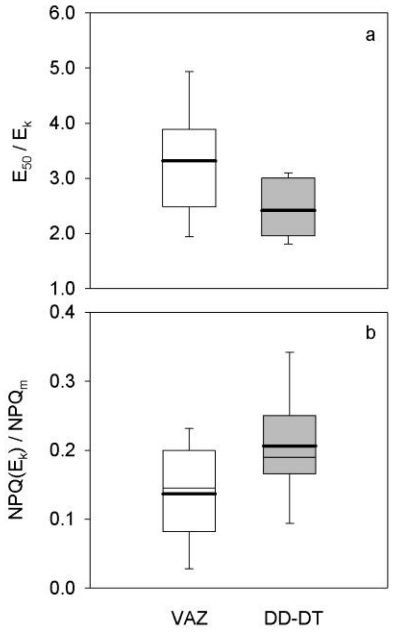

912